# Four-wave mixing of Weyl semimetals in a strong magnetic field

**Yang Gao[iD], Furu Zhang and Wei Zhang[1][iD]**

Institute of Applied Physics and Computational Mathematics, Beijing 100088,
People's Republic of China

E-mail: zhang_wei@iapcm.ac.cn

## Abstract

We theoretically investigate the four-wave mixing process in Weyl semimetals in a strong
magnetic field using quantum theory. Weyl semimetals in a strong magnetic field have an
extremely high third-order nonlinear optical susceptibility (several orders larger than that of the
usual three dimensional materials) originating from the linear energy dispersion near the Weyl
points. The third-order response of Weyl semimetal is nearly independent on the Fermi level,
which is quite different from the sensitive dependence (on the Fermi level) of the linear response.
The unusual polarization dependent selection rules lead to rich nonlinear optical properties,
which can be tuned by the polarization of the incident light fields and the magnetic fields.

(Some figures may appear in colour only in the online journal)

## 1. Introduction

Weyl semimetals are examples of Dirac matter in three dimensions whose band structure has pairs of linearly touching conduction and valence bands [1–5]. The Weyl nodes behave like a source or sink of Berry curvature in momentum space. The Weyl semimetals can be realized from a Dirac system by breaking either time reversal symmetry or inversion symmetry. In recent years, a great deal of attention has been attracted by theoretically predicted and experimentally discovered topological materials, including Weyl semimetals [6–11]. A distinctive feature of Weyl semimetals is the anomalous magnetotransport phenomena related to the chiral anomaly, which has been investigated in high energy physics and condensed matter physics [4, 5, 12–20]. Many studies have shown that the magnetotransport exhibits strong and anisotropic magnetic field dependencies [21–25]. These works have been based on the linear response theory.

With regard to the nonlinear transport and optical response in Weyl semimetals, photocurrent and second harmonic generation were studied by some pioneering works [26–39]. In the absence of external magnetic fields, the photocurrent or second harmonic generation in Weyl semimetals usually involved three mechanisms, the injection current, the shift current, and the anomalous current contributions. Nonlinear anomalous current in Weyl semimetals has been studied in detail in [38]. Under an external weak magnetic field, a photogalvanic effect and the second harmonic generation can be induced in Weyl semimetals and they are linear with the magnetic field. Also, the chiral magnetic effect and the optical activity have contributed to the second nonlinear optical response [30, 31]. Most importantly, the experimental results show that Weyl semimetals show larger nonlinear optical response than any other materials [36]. Also graphene, a two dimensional Dirac material, shows a high optical nonlinearity due to its unusual band structure near the Dirac point [40–43]. It is important to explore the nonlinear optics of three dimensional Weyl semimetals and compare with that of two dimensional Dirac materials.

In this paper, we study the third-order nonlinear optical responses of Weyl semimetals in a strong magnetic field. The employed method is based on the quantum mechanical density matrix formalism [40]. It is found that Weyl semimetals have a very high nonlinear susceptibility for the four-wave-mixing process, and the third-order nonlinear susceptibility is nearly independent on the Fermi level, though the linear absorption spectrum is sensitive to the Fermi level position. With decreasing the external magnetic field or the Fermi velocity of Weyl semimetals, the third order nonlinear susceptibility increases.

The unusual polarization dependent selection rules lead to rich nonlinear optical properties, which can be tuned by the ellipticity (for elliptically polarized lights) and the polarization direction (for linearly polarized incident fields).

## 2. The theoretical formulism, the selection rules and the linear responses

As the basis for studying nonlinear optics, we first present the theoretical formulism, the selection rules and the linear responses.

### 2.1. Landau levels in Wely semimetals

The Hamiltonian for a generic chiral Weyl node can be expressed in momentum space as

$$H_W = \lambda \hbar v_F \boldsymbol{\sigma} \cdot \boldsymbol{k}, \tag{1}$$

where $\lambda = \pm 1$ is chirality index, $v_F$ is the Fermi velocity, $\boldsymbol{\sigma}$ is the vector of Pauli matrices, and $\boldsymbol{k}$ is the momentum relative to the Weyl node. Now we consider a strong magnetic field that is exerted along the $z$ axis, $\boldsymbol{B} = B\hat{z}$. Replacing the momentum $\boldsymbol{p}$ by the kinetic momentum $\boldsymbol{p} \to \boldsymbol{\pi} = \boldsymbol{p} + \frac{e}{c}\boldsymbol{A}^B$, with $\boldsymbol{A}^B = (0, Bx, 0)$, the Hamiltonian becomes

$$H^B = \lambda v_F \boldsymbol{\sigma} \cdot \left( \boldsymbol{p} + \frac{e}{c}\boldsymbol{A}^B \right). \tag{2}$$

By solving the Schrödinger equation $H^B \Psi_n(k, r) = \varepsilon_n(k_z) \Psi_n(k, r)$, it can be found that the Landau levels are given by [25]

$$\varepsilon_n(k_z) = \begin{cases} \mathrm{sgn}(n)\hbar v_F \sqrt{\dfrac{2|n|}{l_B^2} + k_z^2}, & n \neq 0, \\ -\lambda \hbar v_F k_z, & n = 0, \end{cases} \tag{3}$$

where $l_B = \sqrt{\hbar c/eB}$ is magnetic length. And the full expression for eigenstates is

$$\Psi_n(k, r) = \frac{C_n \mathrm{e}^{-\mathrm{i}(k_y y + k_z z)}}{\sqrt{L_y L_z}} \begin{pmatrix} u_n \, \mathrm{sgn}(n) \mathrm{i}^{|n|-1} \phi_{|n|-1} \\ v_n \mathrm{i}^{|n|} \phi_{|n|} \end{pmatrix}, \tag{4}$$

with

$$u_n = \sqrt{\frac{1}{2}\left( 1 + \frac{\hbar v_F k_z}{E_n} \right)}, \quad v_n = \sqrt{\frac{1}{2}\left( 1 - \frac{\hbar v_F k_z}{E_n} \right)}, \tag{5}$$

$$C_n = \begin{cases} 1 & n = 0 \\ \dfrac{1}{\sqrt{2}} & n \neq 0 \end{cases}, \tag{6}$$

$$\phi_{|n|} = \frac{H_n\left( \frac{x - l_B^2 k_y}{l_B} \right)}{\sqrt{2^{|n|} |n|! \sqrt{\pi} l_B}} \exp\left( -\frac{1}{2}\left( \frac{x - l_B^2 k_y}{l_B} \right)^2 \right), \tag{7}$$

and $H_n(x)$ the Hermite polynomial.

A graphic illustration of the Landau levels is shown in figure 1 with the Fermi velocity $v_F = 4.3 \times 10^5 \, \mathrm{m\,s^{-1}}$ and the

magnetic field $B = 10\,\mathrm{T}$ [25, 44]. The $n = 0$ Landau levels are polarized and $n \neq 0$ Landau levels are particle-hole symmetric. The characteristic $n = 0$ Landau levels play an important role in the chiral anomaly in Weyl semimetals. Meanwhile, the structure of the Landau levels controls the shape of the linear absorption coefficient, as we will elaborate it later.

### 2.2. Selection rules and the dipole moment matrix elements

We consider an incident field $\boldsymbol{E}_{L(R)} = E(\omega)\mathrm{e}^{-\mathrm{i}\omega t}\boldsymbol{e}_{L(R)}$ propagating in the $z$ direction. The circular-polarization unit vectors are defined by $\boldsymbol{e}_{L(R)} = \frac{1}{\sqrt{2}}(\boldsymbol{x_0} \pm \mathrm{i}\boldsymbol{y_0})$, where $\boldsymbol{e}_{L/R}$ corresponds to left/right circular polarization. To include the optical field in the Hamiltonian, we introduce its vector potential, $\boldsymbol{E} = (-1/c)\partial \boldsymbol{A}^{\mathrm{opt}}/\partial t$. We consider the case with both a dc magnetic field and an optical field so that the Hamiltonian becomes

$$H = \lambda v_F \boldsymbol{\sigma} \cdot \left( \boldsymbol{p} + \frac{e}{c}\boldsymbol{A}^B + \frac{e}{c}\boldsymbol{A}^{\mathrm{opt}} \right), \tag{8}$$

where $H^{\mathrm{opt}} = \lambda v_F \boldsymbol{\sigma} \cdot \frac{e}{c}\boldsymbol{A}^{\mathrm{opt}}$ is the interaction Hamiltonian. The matrix element of the optical transition between Landau levels is

$$\langle m, k_z' | H^{\mathrm{opt}} | n, k_z \rangle = -\frac{\mathrm{i}\lambda v_F e}{\omega} \langle m | \sigma_x \boldsymbol{x_0} + \sigma_y \boldsymbol{y_0} | n \rangle \delta_{k_z', k_z} \boldsymbol{E}. \tag{9}$$

The dipole moment matrix element can be calculated as

$$\boldsymbol{\mu}_{mn} = \frac{\mathrm{i}\hbar \lambda e v_F}{\varepsilon_{nk} - \varepsilon_{mk'}} \langle m, \boldsymbol{k}' | \sigma_x \boldsymbol{x_0} + \sigma_y \boldsymbol{y_0} | n, \boldsymbol{k} \rangle, \tag{10}$$

where

$$\langle m, k_z' | \sigma_x \boldsymbol{x_0} + \sigma_y \boldsymbol{y_0} | n, k_z \rangle$$
$$= \delta_{k_z', k_z} \sqrt{2} C_m C_n \left( u_m v_n \, \mathrm{sgn}(m) \mathrm{i}^{|n|-|m|+1} \langle \phi_{|m|-1} | \phi_{|n|} \rangle \boldsymbol{e}_L \right.$$
$$\left. + v_m u_n \, \mathrm{sgn}(n) \mathrm{i}^{|n|-|m|-1} \langle \phi_{|m|} | \phi_{|n|-1} \rangle \boldsymbol{e}_R \right). \tag{11}$$
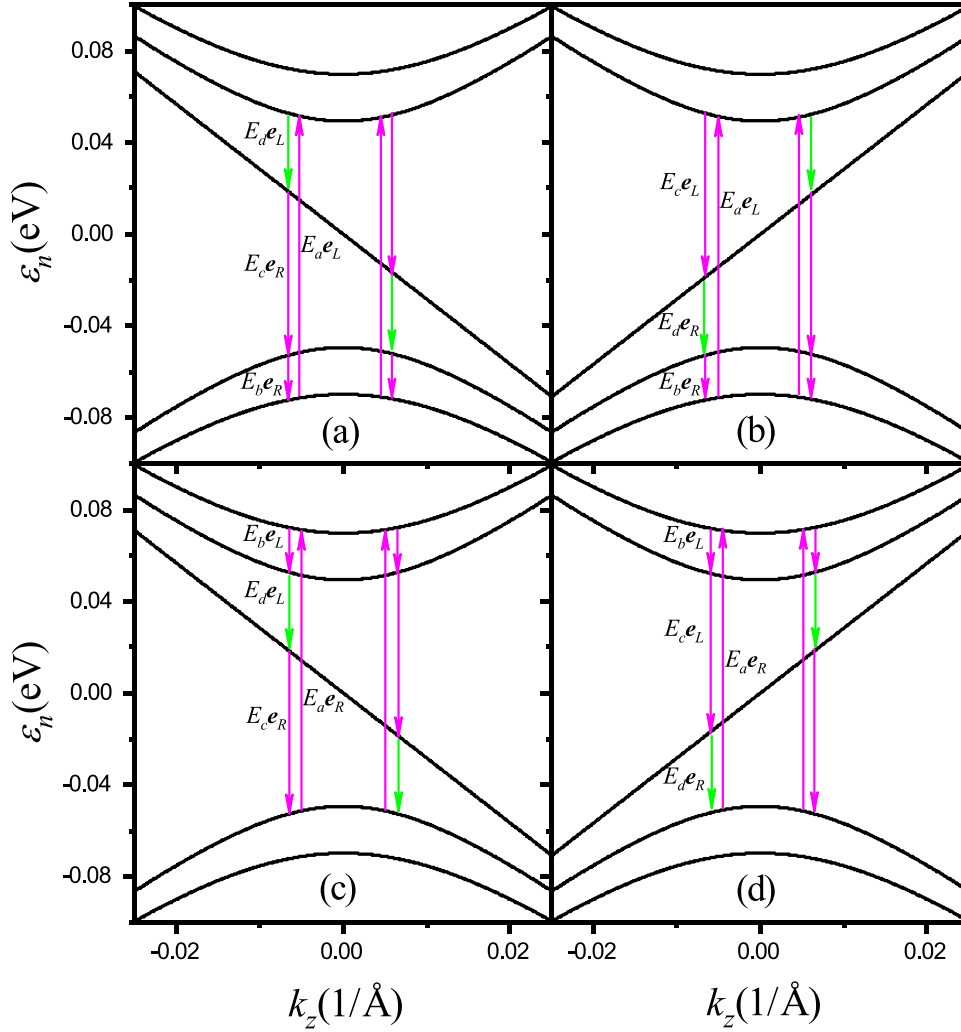
The nonzero matrix element appears when $|m| = |n| - 1$ (for left circularly polarized light) and $|m| = |n| + 1$ (for right circularly polarized light). In other words, the selection rules associated with the left or right-hand circularly polarized light for inter-Landau level transitions are $\Delta |n| = \pm 1$ [25], and not dependent on the chirality of Weyl node. This selection rules for Weyl semimetals in a strong magnetic field are similar to that for two dimensional electrons in graphene [40].

### 2.3. Linear optical responses

The equation of motion of the density matrix is given by

$$\dot{\rho}_{nm} = -\frac{\mathrm{i}}{\hbar}(\varepsilon_n - \varepsilon_m)\rho_{nm}$$
$$\quad - \frac{\mathrm{i}}{\hbar}[H^{\mathrm{opt}}(t), \rho]_{nm} - \gamma_{nm}\left( \rho_{nm} - \rho_{nm}^{(\mathrm{eq})} \right). \tag{12}$$

Here $\rho_{nm}$ denote the elements of the density matrix, and the last term on the right-hand side is the damping term, which indicates that $\rho_{nm}$ relaxes to its equilibrium state $\rho_{nm}^{(\mathrm{eq})}$ at rate $\gamma_{nm}$. In addition, we make the assumption that $\rho_{nm}^{(\mathrm{eq})} = 0$ for $n \neq m$. We

**Figure 1.** The Landau levels in Weyl semimetal and a scheme of the four-wave mixing process in the five-level system of eigenstates with quantum numbers $n = -2, -1, 0, +1, +2$ that were renamed as states $|1\rangle, |2\rangle, |3\rangle, |4\rangle$ and $|5\rangle$ for convenience of notation. Different optical processes are displayed in (a)–(d). The fields $E_i$ ($i = a, b, c, d$) are coupled to electric dipole allowed Landau level transitions. The Fermi velocity $v_F = 4.3 \times 10^5$ m s$^{-1}$ and the magnetic field $B = 10$ T.

will seek a solution to the equation (12) in the form of a perturbation expansion. One thereby obtain the set of equations

$$\dot{\rho}_{nm}^{(0)} = -(i\omega_{nm} + \gamma_{nm})\rho_{nm}^{(0)} + \gamma_{nm}\rho_{nm}^{(eq)}, \quad (13)$$

$$\dot{\rho}_{nm}^{(1)} = -(i\omega_{nm} + \gamma_{nm})\rho_{nm}^{(1)} - \frac{i}{\hbar}[H^{opt}(t), \rho^{(0)}]_{nm}, \quad (14)$$

where $\omega_{nm} = (\varepsilon_n - \varepsilon_m)/\hbar$.

The density matrix $\rho_{nm}^{(1)}(t)$ can be obtained as

$$\rho_{nm}^{(1)}(t) = \frac{1}{\hbar}(\rho_{mm}^{(0)} - \rho_{nn}^{(0)})\sum_{\omega} \frac{\tilde{\mu}_{nm}E(\omega)e^{-i\omega t}}{(\omega_{nm} - \omega) - i\gamma_{nm}}, \quad (15)$$

where

$$\tilde{\mu}_{nm} = \frac{i\lambda v_F e}{\omega}\langle n|\boldsymbol{\sigma}|m\rangle. \quad (16)$$
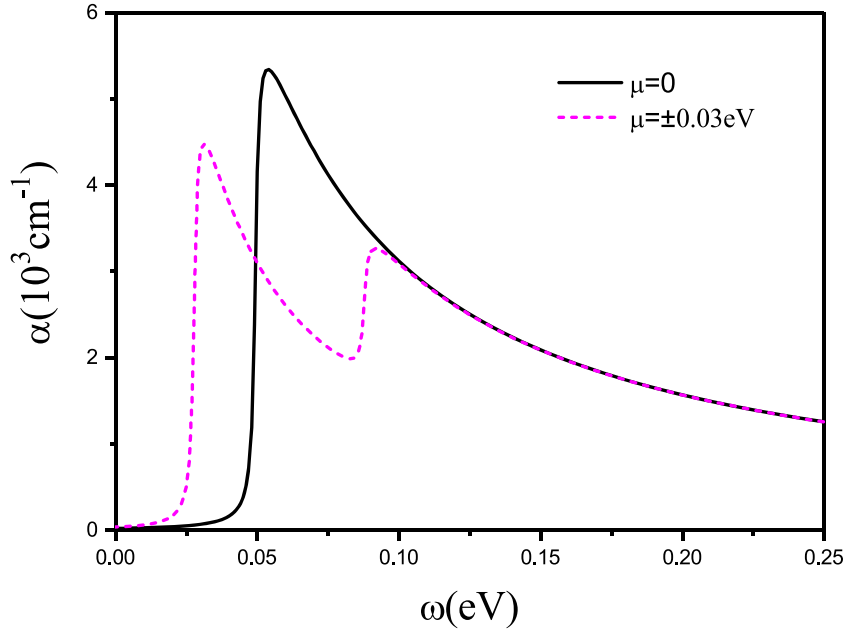
We define the linear polarization in the form

$$\boldsymbol{P}^{(1)}(\omega) = N\,\text{tr}(\rho^{(1)}\boldsymbol{\mu}) = N\sum_{nm}\rho_{nm}^{(1)}\boldsymbol{\mu}_{mn}, \quad (17)$$

We assume the relaxation rates between different Landau levels to be the same $\gamma_{nm} = \gamma$ [45]. One can obtain from equation (17) the linear susceptibility

$$\chi^{(1)}(\omega) = \frac{N}{\epsilon_0}\sum_{nm}[f(\varepsilon_m) - f(\varepsilon_n)]\frac{\boldsymbol{\mu}_{mn}[\tilde{\boldsymbol{\mu}}_{nm} \cdot \boldsymbol{e}]}{(\hbar\omega_{nm} - \hbar\omega) - i\gamma}, \quad (18)$$

here $\rho_{nn}^{(0)}$ follows Fermi distribution $f(\varepsilon_n) = 1/[e^{(\varepsilon_n - \mu)/k_B T} + 1]$. We finally obtain the linear optical susceptibility for the left/right-hand polarizations

$$\chi^{(1)}(\omega, \boldsymbol{e}_L) = \frac{(ev_F)^2}{2\pi^2 l_B^2 \epsilon_0}\int dk_z (C_m C_n u_m v_n)^2$$

$$\times \frac{f(\varepsilon_n) - f(\varepsilon_m)}{\omega\omega_{nm}[(\hbar\omega_{nm} - \hbar\omega) - i\gamma]}\delta_{|n|,|m|-1},$$

$$\chi^{(1)}(\omega, \boldsymbol{e}_R) = \frac{(ev_F)^2}{2\pi^2 l_B^2 \epsilon_0}\int dk_z (C_m C_n u_n v_m)^2$$

$$\times \frac{f(\varepsilon_n) - f(\varepsilon_m)}{\omega\omega_{nm}[(\hbar\omega_{nm} - \hbar\omega) - i\gamma]}\delta_{|m|,|n|-1}. \quad (19)$$

**Figure 2.** The absorption coefficient $\alpha$ as a function of the incident field frequency $\omega$ for the transition between Landau levels $n = 0$ and $n = 1$ at zero temperature. For the Fermi energy $\mu = 0$ there is a broad range of frequencies greater than 50 meV when only the left circular polarization is absorbed. For the Fermi energy $\mu = \pm 30$ meV there are two strong absorption peak. The other parameters are taken as the Fermi velocity $v_F = 4.3 \times 10^5$ m s$^{-1}$, the magnetic field $B = 10$ T, the relaxation constant $\gamma = 1$ meV.

The absorption coefficient can be expressed as

$$\alpha = \frac{\omega}{c} \, \text{Im}[\chi^{(1)}(\omega)]. \tag{20}$$

For the comparison with the nonlinear optical responses, the linear absorption coefficient for the transition between Landau levels $n = 0$ and $n = 1$ at zero temperature is shown in figure 2. One asymmetric peak of the absorption coefficient with the incident frequency can be seen when the Fermi energy $\mu = 0$[solid black curve], which comes from the dispersive structure of the Landau levels. Moreover, the absorption frequency bandwidth can be tuned by adjusting the external magnetic fields or Fermi levels position. The Fermi levels for the two opposite chiralities shift $\pm 30$ meV when a constant electric field is applied parallel to the magnetic field. It is interesting to observe that there exist two peaks of the absorption coefficient, this method can used for the detection of the chiral anomaly [25, 44]. With increasing the incident optical frequency, a series of absorption peaks have emerged corresponds to allowed interband transitions in the Landau level structure [25].

## 3. The third-order optical responses

### 3.1. The resonant four-wave mixing

Let us now consider the four-wave-mixing process shown in figure 1. We take the optical process in figure 1(a) as an example. The total field consists of the four waves: three pump fields at frequencies $\omega_a$, $\omega_b$ and $\omega_c$ resonant to the corresponding transitions between the Landau levels $|1\rangle \to |4\rangle$, $|2\rangle \to |1\rangle$ and $|3\rangle \to |2\rangle$, and one circular polarization signal field at frequency $\omega_d = \omega_a - \omega_b - \omega_c$ nearly resonant with the transition

from $|4\rangle$ to $|3\rangle$. The pumping fields are of the form

$$\boldsymbol{E} = \boldsymbol{e}_L E_a \text{e}^{-\text{i}\omega_a t} + \boldsymbol{e}_R E_b \text{e}^{-\text{i}\omega_b t} + \boldsymbol{e}_R E_c \text{e}^{-\text{i}\omega_c t}. \tag{21}$$

We introduce the slowly varying quantity $\sigma_{nm}$, defined by $\rho_{41} = \sigma_{41} \text{e}^{-\text{i}\omega_a t}$, $\rho_{43} = \sigma_{43} \text{e}^{-\text{i}\omega_d t}$, $\rho_{32} = \sigma_{32} \text{e}^{-\text{i}\omega_c t}$ and $\rho_{21} = \sigma_{21} \text{e}^{-\text{i}\omega_b t}$. In terms of these new quantities, equation (12) becomes

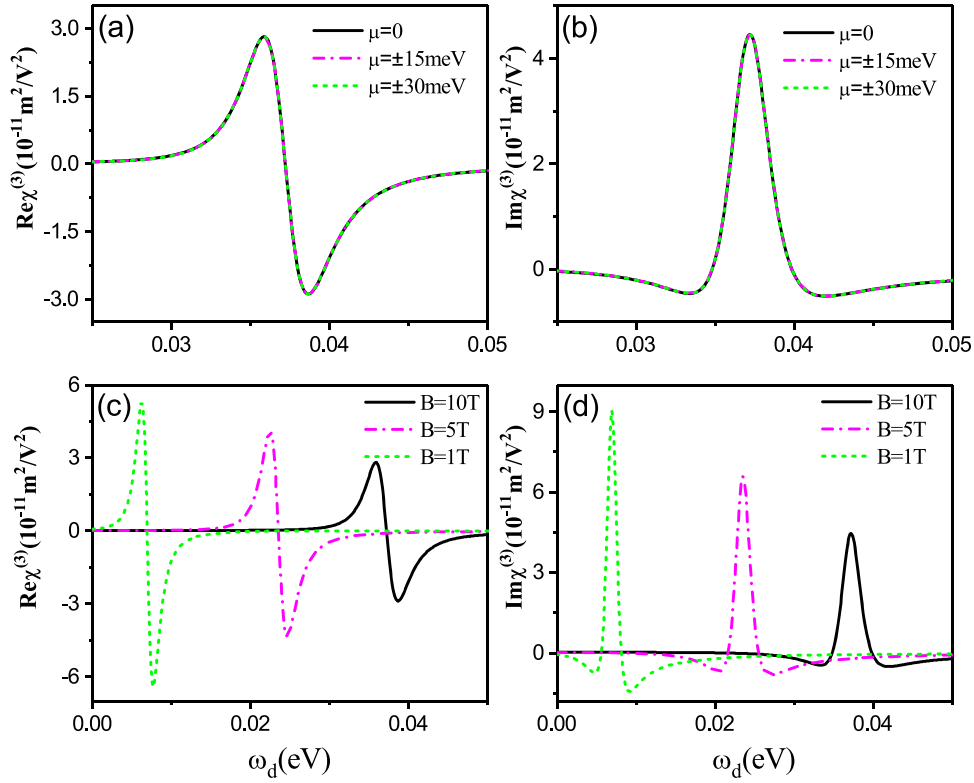$$\dot{\sigma}_{nm} + \Gamma_{nm}\sigma_{nm} = -\frac{i}{\hbar}[H^{\text{opt}}(t), \rho]_{nm}, \tag{22}$$

where the complex de-phasing $\Gamma_{nm} = \gamma_{nm} + \text{i}(\omega_{nm} - \omega_j)$, $j = a, b, c, d$. We assume that all detunings from resonance are small. The equations of motion for the density matrix elements are given explicitly as

$$\dot{\sigma}_{43} + \Gamma_{43}\sigma_{43} = i\Omega_{41}\sigma_{31}^* - i\Omega_{32}^*\sigma_{42};$$

$$\dot{\sigma}_{32} + \Gamma_{32}\sigma_{32} = i\Omega_{32}(\rho_{22} - \rho_{33}) - i\Omega_{21}^*\sigma_{31};$$

$$\dot{\sigma}_{41} + \Gamma_{41}\sigma_{41} = i\Omega_{41}(\rho_{11} - \rho_{44}) - i\Omega_{21}\sigma_{42};$$

$$\dot{\sigma}_{21} + \Gamma_{21}\sigma_{21} = i\Omega_{21}(\rho_{11} - \rho_{22}) + i\Omega_{32}^*\sigma_{31} - i\Omega_{41}\sigma_{42}^*; \tag{23}$$

$$\dot{\sigma}_{31} + \Gamma_{31}\sigma_{31} = -i\Omega_{21}\sigma_{32} - i\Omega_{41}\sigma_{43}^* + i\Omega_{32}\sigma_{21};$$

$$\dot{\sigma}_{42} + \Gamma_{42}\sigma_{42} = -i\Omega_{21}^*\sigma_{41} - i\Omega_{32}\sigma_{43} + i\Omega_{41}\sigma_{21}^*,$$

where $\Omega_{nm} = \tilde{\boldsymbol{\mu}}_{nm} \cdot \boldsymbol{E}_{nm}/\hbar$ is the on-resonance Rabi frequency, and the field amplitude are $\boldsymbol{E}_{21} = \boldsymbol{E}_b$, $\boldsymbol{E}_{32} = \boldsymbol{E}_c$ and $\boldsymbol{E}_{41} = \boldsymbol{E}_a$. The steady state solution can be obtained by setting $\dot{\sigma}_{nm} = 0$ in equation (23).

In the four-wave-mixing process shown in figure 1, the complex amplitude of the component of the nonlinear polarization oscillating at frequency $\omega_d$ is given by

$$\boldsymbol{P}(\omega_d) = N \cdot \boldsymbol{\mu}_{43}\sigma_{43}\text{e}^{-\text{i}\omega_d t} + c.c. \tag{24}$$

**Figure 3.** The real and imaginary parts of the third-order nonlinear susceptibility $\chi_{43}^{(3)}(\omega_d)$ as a function of the output frequency $\omega_d$ for different Fermi levels $\mu$ at $B = 10$ T [(a) and (b)] and for different magnetic field $B$ at $\mu = 0$ [(c) and (d)]. The other parameters are taken as the Fermi velocity $v_F = 4.3 \times 10^5$ m s$^{-1}$, $\gamma = 1$ meV.

By combining equations (23) and (24), we find that the third order susceptibility is given by

$$\chi_{43}^{(3)}(\omega_d) = \frac{i^3 N}{\hbar^3 \epsilon_0} \sum_{1,2,3,4} \boldsymbol{\mu}_{43} \frac{\tilde{\boldsymbol{\mu}}_{41} \tilde{\boldsymbol{\mu}}_{32}^* \tilde{\boldsymbol{\mu}}_{21}^*}{\Gamma_{43}} \left( -\frac{\rho_{22} - \rho_{33}}{\Gamma_{32}^* \Gamma_{31}^*} \right.$$
$$\left. + \frac{\rho_{11} - \rho_{22}}{\Gamma_{31}^* \Gamma_{21}^*} + \frac{\rho_{11} - \rho_{44}}{\Gamma_{42} \Gamma_{41}} + \frac{\rho_{11} - \rho_{22}}{\Gamma_{42} \Gamma_{21}^*} \right).$$

(25)

Here we keep only the terms leading to the third-order nonlinear susceptibility corresponding to the four-wave-mixing (see figure 1).

In general, the diagonal elements of the matrix density, i.e., the populations of the levels are determined by the Fermi level, which can be tuned by the external field [46, 47]. We assume the Fermi level is between the landau level $n = -1$ and landau level $n = 1$, which means $\rho_{11} = \rho_{22} = 1$, $\rho_{33} = f(\varepsilon_0) = 1/[e^{(\varepsilon_0 - \mu)/k_B T} + 1]$ and $\rho_{44} = 0$.
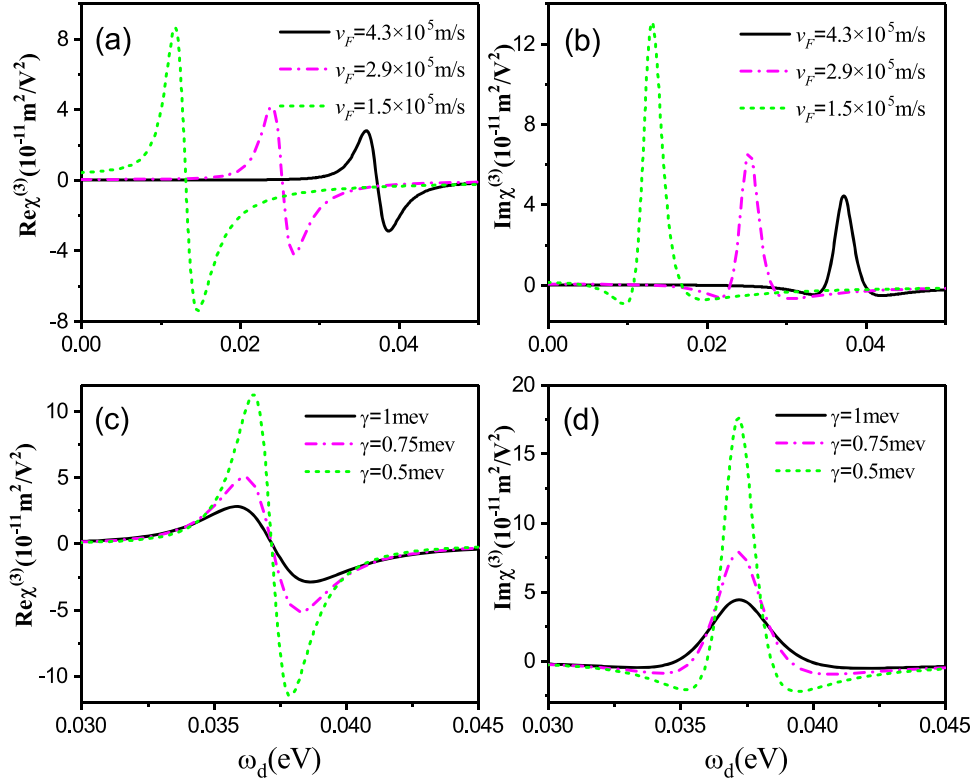
In the four-wave-mixing process, there is no contribution for the transition $|2\rangle \to |1\rangle$ because states $|1\rangle$ and $|2\rangle$ are fully occupied. Changing from summation to integration, we find that the third order susceptibility $\chi_{43}^{(3)}$ is further simplified to

$$\chi_{43}^{(3)}(\omega_d) = \frac{i^3 N}{\hbar^3 \epsilon_0} \int \frac{\mathrm{d}k_z}{2\pi} \boldsymbol{\mu}_{43} \frac{\tilde{\boldsymbol{\mu}}_{41} \tilde{\boldsymbol{\mu}}_{32}^* \tilde{\boldsymbol{\mu}}_{21}^*}{\Gamma_{43}}$$
$$\times \left( -\frac{1 - f(\varepsilon_0)}{\Gamma_{32}^* \Gamma_{31}^*} + \frac{1}{\Gamma_{42} \Gamma_{41}} \right). \quad (26)$$

Equation (26) can be used in the four-wave mixing process near the Weyl nodes and away from the band bottom of zero Landau band in the two-node model [46]. This results also apply for three-dimensional Dirac semimetals.

### 3.2. Modulation of the four-wave mixing

Firstly, we analyze the effects of external fields on the nonlinear optics property of Weyl semimetal systems. We know that Landau levels can be adjusted by external magnetic fields $\boldsymbol{B}$ and the effective Fermi levels can be adjusted by a constant electric field $\boldsymbol{E} \| \boldsymbol{B}$. Figure 3 shows the output frequency dependence of $\chi_{43}^{(3)}$ in different other parameters which satisfy the frequency and phase matching condition. From figures 3(a) and (b), one can see that the real and imaginary parts of $\chi_{43}^{(3)}$ exhibit a resonance at $\omega_d = \omega_a - \omega_b - \omega_c \approx 37$ meV when the magnetic field $B = 10$ T, the Fermi energy $\mu = 0$ and the relaxation constant $\gamma = 1$ meV. The real and imaginary parts of $\chi_{43}^{(3)}$ exhibition positive and negative amplitudes because of the complex denominator function $\Gamma_{nm}$ contribution to the nonlinear processes. Importantly, the absolute value of $\chi_{43}^{(3)}$ is several orders of magnitude larger than any bulk material we know [48]. Similarly, graphene, a two dimensional Dirac material, in a strong magnetic field also has the extremely strong optical nonlinearity [40–43]. The third order nonlinear susceptibility $\chi_{43}^{(3)}$ is different from the linear absorption coefficient $\alpha$, where $\alpha$ depends on the Fermi levels for the two opposite chiralities (see figure 2). As seen from figures 3(a) and (b), the $\chi_{43}^{(3)}$

**Figure 4.** The third-order nonlinear susceptibility $\chi_{43}^{(3)}$ as a function of the output frequency $\omega_d$ for different Fermi velocity $v_F$ at $\gamma = 1$ meV [(a) and (b)] and for different relaxation constant $\gamma$ at $v_F = 4.3 \times 10^5$ m s$^{-1}$ [(c) and (d)]. The other parameters are taken as $B = 10$ T, $\mu = 0$.

is nearly independent on the Fermi level showing stable non-linear optics property. Figures 3(c) and (d) show that when the Fermi levels $\mu$ and relaxation constant $\gamma$ are fixed, the resonant peaks of nonlinear susceptibility $\chi_{43}^{(3)}$ shifted to lower frequencies as a consequence of the decrease of the energy spacing between the Landau levels. Additionally, one can find that the absolute value of $\chi_{43}^{(3)}$ increases with the decrease of magnetic field.

Figures 4(a) and (b) show the output frequency dependence of the third order nonlinear susceptibility for the different Fermi velocity. Because of anisotropy, the Fermi velocity $v_F$ covers a wide range in real Weyl semimetals [49]. When decreasing the Fermi velocity, the resonant peaks of nonlinear susceptibility shifted to lower frequencies since the energy between the Landau levels reduces. Moreover, the third order nonlinear susceptibility peak shows an obvious rise because of the enhancing of the complex denominator function $\Gamma_{nm}$ contribution to the nonlinear processes (see equation (26)). The output frequency dependence of the nonlinear susceptibility for different relaxation constant $\gamma$ is shown in figures 4(c) and (d). With decreasing the relaxation constant, the resonant peaks in the nonlinear susceptibility increase. This is a universal phenomenon of the actual relaxation dynamics of electrons [50, 51]. Also the negative imaginary part becomes more obvious.

From the above analysis, a strong optical nonlinearity could be achieved for small external magnetic field and Fermi velocity. Compared with the experimental results in literatures, the external magnetic field $B = 1$ T, $\hbar v_F \sim 1 - 10$ eV Å in

Bi$_{0.97}$Sb$_{0.03}$ and Cd$_3$As$_2$ [49]. Taking a reasonable value for the dephasing rate $\gamma = 1$ meV [25], the third order nonlinear susceptibility $\chi_{43}^{(3)} \sim 10^{-10} - 10^{-9}$ m$^2$ V$^{-2}$. This result is surprisingly high, perhaps the highest among known three dimensional materials.

The nonlinear optical response can be modulated not only by the magnetic field, but also by the frequency and polarization of the incident fields. Unlike the two-dimensional graphene, where the Landau levels are flat, the Landau levels in three-dimensional Weyl semimetals are dispersive, thus it is possible to tune the resonant four-wave mixing by changing the frequencies of the incident fields. Moreover, the polarization plays an important role in the nonlinear responses due to the polarization dependent selection rules. In general, the pump fields are of the form

$$
\begin{aligned}
\boldsymbol{E}_j &= [\cos(\alpha_j)\boldsymbol{x}_0 + \mathrm{e}^{\mathrm{i}\delta_j} \sin(\alpha_j)\boldsymbol{y}_0]E_0\mathrm{e}^{\mathrm{i}\omega_j t - k_z z} \\
&= \frac{1}{\sqrt{2}} [(\cos(\alpha_j) - i\mathrm{e}^{\mathrm{i}\delta_j} \sin(\alpha_j))\boldsymbol{e}_\mathrm{L} \\
&\quad + (\cos(\alpha_j) - i\mathrm{e}^{\mathrm{i}\delta_j} \sin(\alpha_j))\boldsymbol{e}_\mathrm{R}] E_0\mathrm{e}^{\mathrm{i}\omega_j t - k_z z}, \quad (27)
\end{aligned}
$$

where $j = a, b, c$. Our calculation shows that the out put field

$$
\begin{aligned}
\boldsymbol{E}_d &\propto [\cos(\alpha_a)\cos(\alpha_b) + \mathrm{e}^{\mathrm{i}(\delta_a + \delta_b)} \sin(\alpha_a)\sin(\alpha_b)] \\
&\quad \times [(\cos(\alpha_c) + i\mathrm{e}^{\mathrm{i}\delta_c} \sin(\alpha_c))\boldsymbol{e}_\mathrm{L} \\
&\quad + (\cos(\alpha_c) - i\mathrm{e}^{\mathrm{i}\delta_c} \sin(\alpha_c))\boldsymbol{e}_\mathrm{R}]. \quad (28)
\end{aligned}
$$

It is seen that the polarization of the output field $E_d$ is determined by the polarization of the field $E_c$. The intensity of the signal field $E_d$ (with frequency $\omega_d$) is of the form of

$$
\begin{aligned}
I_d \propto\ & 2\,\cos(\alpha_a)\cos(\alpha_b)\sin(\alpha_a)\sin(\alpha_b)\cos(\delta_a + \delta_b) \\
& + \cos^2(\alpha_a)\cos^2(\alpha_b) + \sin^2(\alpha_a)\sin^2(\alpha_b),
\end{aligned} \quad (29)
$$

which can by tuned by changing the polarizations of the fields $E_a$, $E_b$. For the linear polarization with $\delta_a = \delta_b = 0$, the intensity $I_d \propto \cos^2(\alpha_a - \alpha_b)$, depending on the polarization direction difference of the incident fields $E_a$ and $E_b$. In particular, $I_d$ vanishes when the polarization direction $E_a$ perpendular to that of $E_b$. While for the elliptically polarized pump fields with $\delta_a = \delta_b = \pi/2$, $I_d \propto \cos^2(\alpha_a + \alpha_b)$. If $\alpha_a = \alpha_b = \pi/4$ (i.e., both fields are left circularly polarized), $I_d = 0$ as a consequence of selection rules (see figure 1). While for $\alpha_a = -\alpha_b$ (i.e., the two fields with opposite handness of the polarization), the maximum output field can be obtained. These rich polarization dependent nonlinear optical properties are due to the particular selection rules.

## 4. Conclusion

In summary, we have studied the linear and nonlinear optical response of Weyl semimetals in a strong magnetic field. We have obtained analytic formulas for the third-order nonlinear susceptibility and found that the system has a high optical nonlinearity. While the linear absorption spectrum depends upon Fermi level position of the Weyl semimetals, it has little effect on the third-order nonlinear susceptibility. As the Fermi velocity decreases, the third-order nonlinear susceptibility increases. In addition, the nonlinear response can be modulated by polarization of the pump light fields and magnetic fields.

## ORCID iDs

Yang Gao ![ORCID] https://orcid.org/0000-0001-5631-3768
Wei Zhang ![ORCID] https://orcid.org/0000-0002-0284-9396

## References

[1] Murakami S 2007 *New J. Phys.* **9** 356
[2] Wan X, Turner A M, Vishwanath A and Savrasov S Y 2011 *Phys. Rev. B* **83** 205101
[3] Yang K Y, Lu Y M and Ran Y 2011 *Phys. Rev. B* **84** 075129
[4] Burkov A A and Balents L 2011 *Phys. Rev. Lett.* **107** 127205
[5] Xu G, Weng H, Wang Z, Dai X and Fang Z 2011 *Phys. Rev. Lett.* **107** 186806
[6] Neupane M, Richardella A, Sanchez-Barriga J, Xu S Y, Alidoust N, Belopolski I, Liu C, Bian G, Zhang D, Marchenko D, Varykhalov A, Rader O, Leandersson M, Balasubramanian T, Chang T R, Jeng H T, Basak S, Lin H, Bansil A, Samarth N and Hasan M Z 2014 *Nat. Commun.* **5** 3841
[7] Xu S Y, Belopolski I, Alidoust N, Neupane M, Bian G, Zhang C, Sankar R, Chang G, Yuan Z, Lee C C, Huang S M, Zheng H, Ma J, Sanchez D S, Wang B, Bansil A, Chou F, Shibayev P P, Lin H, Jia S and Hasan M Z 2015 *Science* **349** 613
[8] Lv B Q, Weng H M, Fu B B, Wang X P, Miao H, Ma J, Richard P, Huang X C, Zhao L X, Chen G F, Fang Z, Dai X, Qian T and Ding H 2015 *Phys. Rev. X* **5** 031013
[9] Huang X, Zhao L, Long Y, Wang P, Chen D, Yang Z, Liang H, Xue M, Weng H, Fang Z, Dai X and Chen G 2015 *Phys. Rev. X* **5** 031023
[10] Zhang C L, Xu S Y, Belopolski I, Yuan Z, Lin Z, Tong B, Bian G, Alidoust N, Lee C C, Huang S M, Chang T R, Chang G, Hsu C H, Jeng H T, Neupane M, Sanchez D S, Zheng H, Wang J, Lin H, Zhang C, Lu H Z, Shen S Q, Neupert T, Hasan M Z and Jia S 2016 *Nat. Commun.* **7** 10735
[11] Li Q, Kharzeev D E, Zhang C, Huang Y, Pletikosic I, Fedorov A V, Zhong R D, Schneeloch J A, Gu G D and Valla T 2016 *Nat. Phys.* **12** 550
[12] Adler S 1969 *Phys. Rev.* **177** 2426
[13] Bell J S and Jackiw R 1969 *Nuovo Cimento* A **60** 47
[14] Jackiw R 1984 *Phys. Rev.* D **29** 2375
[15] Haldane F D M 1988 *Phys. Rev. Lett.* **61** 2015
[16] Xiao D, Chang M C and Niu Q 2010 *Rev. Mod. Phys.* **82** 1959
[17] Zyuzin A A and Burkov A A 2012 *Phys. Rev. B* **86** 115133
[18] Son D T and Spivak B Z 2013 *Phys. Rev. B* **88** 104412
[19] Burkov A A 2015 *J. Phys.: Condens. Matter* **27** 113201
[20] Wan B, Schindler F, Wang K, Wu K, Wan X, Neupert T and Lu H Z 2018 *J. Phys.: Condens. Matter* **30** 505501
[21] Ashby P E C and Carbotte J P 2013 *Phys. Rev. B* **87** 245131
[22] Burkov A A 2014 *Phys. Rev. Lett.* **113** 247203
[23] Spivak B Z and Andreev A V 2016 *Phys. Rev. B* **93** 085107
[24] Sun Y and Wang A M 2017 *Phys. Rev. B* **96** 085147
[25] Long Z Q, Wang Y R, Erukhimova M, Tokman M and Belyanin A 2018 *Phys. Rev. Lett.* **120** 037403
[26] Deyo E, Golub L E, Ivchenko E L and Spivak B 2009 Semiclassical theory of the photogalvanic effect in non-centrosymmetric systems (arXiv:0904.1917)
[27] Sodemann I and Fu L 2015 *Phys. Rev. Lett.* **115** 216806
[28] Morimoto T and Nagaosa N 2016 *Sci. Adv.* **2** e1501524
[29] Morimoto T, Zhong S, Orenstein J and Moore J E 2016 *Phys. Rev. B* **94** 245121
[30] Cortijo A 2016 *Phys. Rev. B* **94** 235123
[31] Zyuzin A A and Zyuzin A Y 2017 *Phys. Rev. B* **95** 085127
[32] Juan F D, Grushin A G, Morimoto T and Moore J E 2017 *Nat. Commun.* **8** 15995
[33] Chan C K, Lindner N H, Refael G and Lee P A 2017 *Phys. Rev. B* **95** 041104(R)
[34] König E J, Xie H Y, Pesin D A and Levchenko A 2017 *Phys. Rev. B* **96** 075123
[35] Golub L E, Ivchenko E L and Spivak B Z 2017 *JETP Lett.* **105** 782
[36] Wu L, Patankar S, Morimoto T, Nair N L, Thewalt E, Little A, Analytis J G, Moore J E and Orenstein J 2017 *Nat. Phys.* **13** 350
[37] Ma Q, Xu S Y, Chan C K, Zhang C L, Chang G, Lin Y, Xie W, Palacios T, Lin H, Jia S, Lee P A, Herrero P J and Gedik N 2017 *Nat. Phys.* **13** 842
[38] Rostami H and Polini M 2018 *Phys. Rev. B* **97** 195151
[39] Li Z, Jin Y Q, Tohyama T, Iitaka T, Zhang J X and Su H 2018 *Phys. Rev. B* **97** 085201

[40] Yao X and Belyanin A 2012 *Phys. Rev. Lett.* **108** 255503
[41] Yao X and Belyanin A 2013 *J. Phys.: Condens. Matter* **25** 054203
[42] Tokman M, Yao X and Belyanin A 2013 *Phys. Rev. Lett.* **110** 077404
[43] Kutayiah A R, Tokman M, Wang Y and Belyanin A 2018 *Phys. Rev. B* **98** 115410
[44] Ashby P E C and Carbotte J P 2014 *Phys. Rev. B* **89** 245121
[45] Mikhailov S A 2016 *Phys. Rev. B* **93** 085403
[46] Lu H Z, Zhang S B and Shen S Q 2015 *Phys. Rev. B* **92** 045203
[47] Burkov A A 2018 *Annu. Rev. Condens. Matter Phys.* **9** 359
[48] Boyd R W 2008 *Nonlinear Optics* (Amsterdam: Elsevier Science) p 212
[49] Lu H Z and Shen S Q 2015 *Phys. Rev. B* **92** 035203
[50] Cheng J L, Vermeulen N and Sipe J E 2015 *Phys. Rev. B* **91** 235320
[51] Funk H, Knorr A, Wendler F and Malic E 2015 *Phys. Rev. B* **92** 205428